Korean J Physiol Pharmacol
Vol 12: 307−314, December, 2008

Functional Connectivity Map of Retinal Ganglion Cells for Retinal Prosthesis

Jang Hee Ye[1,3], Sang Baek Ryu[2,3], Kyung Hwan Kim[2,3], and Yong Sook Goo[1,3]

[1]Department of Physiology, Chungbuk National University School of Medicine, Cheongju 361-763, [2]Department of Biomedical Engineering, College of Health Science, Yonsei University, Wonju 220-710, [3]Nano Artificial Vision Research Center, Seoul National University Hospital, Seoul 110-744, Korea

Retinal prostheses are being developed to restore vision for the blind with retinal diseases such as retinitis pigmentosa (RP) or age-related macular degeneration (AMD). Among the many issues for prosthesis development, stimulation encoding strategy is one of the most essential electrophysiological issues. The more we understand the retinal circuitry how it encodes and processes visual information, the greater it could help decide stimulation encoding strategy for retinal prosthesis. Therefore, we examined how retinal ganglion cells (RGCs) in in-vitro retinal preparation act together to encode a visual scene with multielectrode array (MEA). Simultaneous recording of many RGCs with MEA showed that nearby neurons often fired synchronously, with spike delays mostly within 1 ms range. This synchronized firing - narrow correlation - was blocked by gap junction blocker, heptanol, but not by glutamatergic synapse blocker, kynurenic acid. By tracking down all the RGC pairs which showed narrow correlation, we could harvest 40 functional connectivity maps of RGCs which showed the cell cluster firing together. We suggest that finding functional connectivity map would be useful in stimulation encoding strategy for the retinal prosthesis since stimulating the cluster of RGCs would be more efficient than separately stimulating each individual RGC.

Key Words: Retinal prosthesis, Retinal ganglion cell, Multielectrode array, Narrow correlation, Functional connectivity map

INTRODUCTION

Retinal prostheses are being developed to restore vision for the blind with retinal diseases such as retinitis pigmentosa (RP) or age-related mucular degeneration (AMD) (Humayun et al, 2003; Rizzo et al, 2003; Zrenner et al, 2006). While the retinal degenerations result in photoreceptor loss, significant numbers of bipolar and ganglion cells remain for many years. Preservation of the inner retinal neurons raises the possibility that appropriate stimulation of these cells with prosthesis may produce vision. (Lowenstein et al, 2004). However, major issues still remain for successful prosthesis development such as inner retinal cell viability, stimulus threshold and safety limit, stimulation encoding, power requirements, biocompatibility, and testing of implant subjects, etc (Lowenstein et al, 2004).

The more we understand the retinal circuitry how it encodes and processes visual information, it is expected to greatly help decide stimulation encoding strategy for retinal prosthesis. Since the retinal ganglion cells (RGCs) are the output cells of the retina, simultaneous recording of the multiple signals carried by a number of RGCs can be a great help to understand the visual information encoding in retina. Multielectrode array (MEA) technology has been established as a powerful tool for simultaneous recording of many neurons in different types of preparations (Meister et al, 1994; Egert et al, 1998; Guenther et al, 2006).

One of the interesting features in the retinal circuit is that there are about 10^8 photoreceptors, hundred times more than ganglion cells, and this implies that the information generated from the photoreceptors are being compressed to a great degree into the small-numbered ganglion cell activities (Meister, 1996; Meister & Berry, 1999). Simultaneous recording of many RGCs with a MEA showed that nearby neurons often fired synchronously, with spike delays of less than 10 miliseconds (Meister et al, 1995; Brivanlou et al, 1998; DeVries 1999). This means that RGCs can hardly function as independent channels for visual information processing. Instead, they somehow signal in a concerted fashion to convey visual information (Meister, 1996; Meister & Berry, 1999).

Many studies have been performed regarding the physiological significance of synchronized firing of RGCs in the visual information processing (Meister et al, 1995; Brivanlou et al, 1998; DeVries, 1999). Nevertheless, little effort has been paid to this synchronized firing as a poten-

Corresponding to: Yong Sook Goo, Department of Physiology, Chungbuk National University School of Medicine, 410, Sungbong-Ro, Cheongju 361-763, Korea. (Tel) 82-43-261-2870, (Fax) 82-43-272-1603, (Email) ysgoo@chungbuk.ac.kr

ABBREVIATIONS: RP, retinitis pigmentosa; AMD, age-related macular degeneration; RGC, retinal ganglion cell; MEA, multielectrode array; ACSF, artificial cerebrospinal fluid; PSTH, post-stimulus time histogram; STA, spike-triggered average.

tial tool for stimulation encoding strategy for the retinal prosthesis. Since some RGCs fire in a concerted manner, it would be efficient than separately stimulating each RGCs, if we can find and stimulate the cluster of RGCs firing together. To address this issue, we introduced an MEA to record spike trains of 1,155 RGCs and found 160 pairs of RGCs showing synchronized firing in an isolated rabbit retina (number of rabbits=18, number of retinas=33).

The rabbit retina is well suited to in vitro recordings with an MEA because it is thin and avascular. In addition, the responses of rabbit RGCs have extensively been characterized in both single electrode (Amthor et al, 1989a, b; Caldwell & Daw, 1978) and paired or multielectrode recordings (Arnett & Spraker, 1981; DeVries & Baylor, 1997; DeVries, 1999). By grouping the synchronously firing RGCs, we were able to draw the functional connectivity map of RGCs (number of maps=40). Some of the preliminary results have been reported in Seo et al (2007).

METHODS

In vitro recording of retinal activity

New Zealand white rabbits (body weight: ~2 kg) were kept overnight in darkness. All subsequent manipulations were done under dim red light to maintain the retina in a dark-adapted state. The method used by Stett et al (2000) was modified for retinal preparation. Briefly, the eyeball was enucleated and the retina was isolated. A retinal segment (~5×5 mm) was mounted to the ganglion cell side on the surface of the MEA. Most recordings were obtained from the central retina, slightly below the visual streak. The retinal preparation was maintained in an artificial cerebrospinal fluid (ACSF) solution (124 mM NaCl, 10 mM glucose, 1.15 mM KH_2PO_4, 25 mM $NaHCO_3$, 1.15 mM $MgSO_4$, 2.5 mM $CaCl_2$, and 5 mM KCl) bubbled with 95 % O_2+5 %CO_2 at pH of 7.3~7.4 and 32°C.

All pharmacological agents were dissolved in an oxygenated ACSF solution and delivered to the retina by continuous perfusion of the ACSF at a rate of 1 ml/min. The glutamatergic synapse blocking was achieved by kynurenic acid (100 μM). The gap junction blocker, heptanol (1 mM) was used to block narrow correlation.

Electrode and data recording system

The MEA60 system (Multi Channel Systems GmbH, Germany) included electrode array, stimulator (STG1004), amplifier (MEA1060), temperature control units, data acquisition hardware (Mc_Card) and software (Mc_Rack). The electrode array had 60 active electrodes in an 8×8 grid layout with electrode diameters of 30 μm and inter-electrode distances of 200 μm and coated with porous titanium nitride (TiN) to minimize electrical impedance. The impedance level was approximately 50 kohm at 1 kHz. The amplifier was placed in a Faraday cage connected to a laboratory-made ground system. Multielectrode recordings of the retinal activity were obtained from 60 electrode channels with a bandwidth, ranging from 10 to 3,000 Hz, at a gain of 1,200. The data sampling rate was 25 kHz/channel.

Light stimulation

For characterization of the RGCs as ON, OFF, or ON/OFF cell, we applied full-field illumination of white light (intensity 1.45 $\mu W/cm^2$) as 2 sec ON and 5 sec OFF protocol for 10 minutes. The retina was stimulated with light stimulus by beam projector, the screen of which was imaged to fit onto the MEA through a microscope (Nikon diaphot, Japan). The light stimulus was made by custom-made software. The setup is illustrated in Fig. 1.

Determination of receptive field of RGC

Ganglion cell receptive field profiles were determined by analyzing responses to random flicker stimulation (Meister et al, 1994; DeVries & Baylor, 1997; Brown et al, 2000). The flickering checkerboard stimulus was composed of 8×8 pixels to align the MEA (200 μm on a side). Each pixel's intensity was either 0 (black flash) or 1 (white flash) accord-

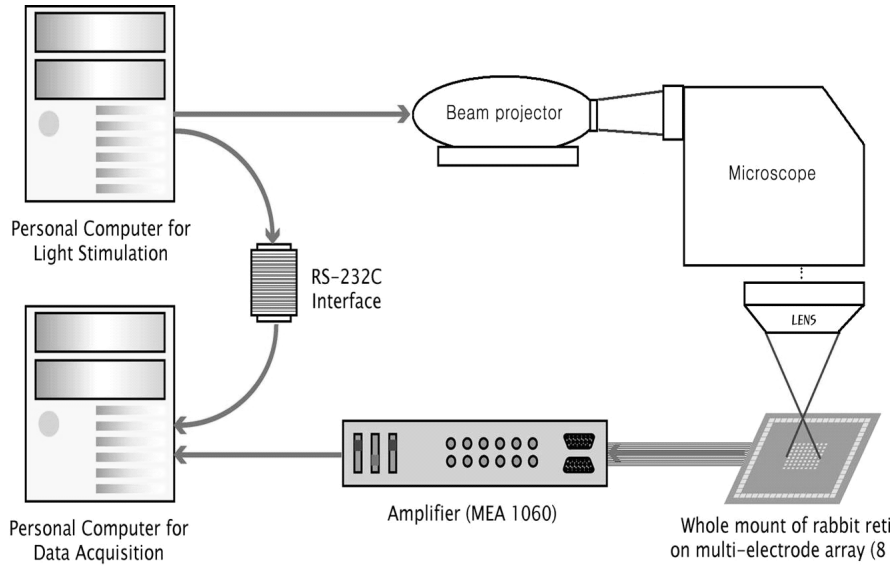

Fig. 1. Schematic diagram of light stimulation and data acquisition.

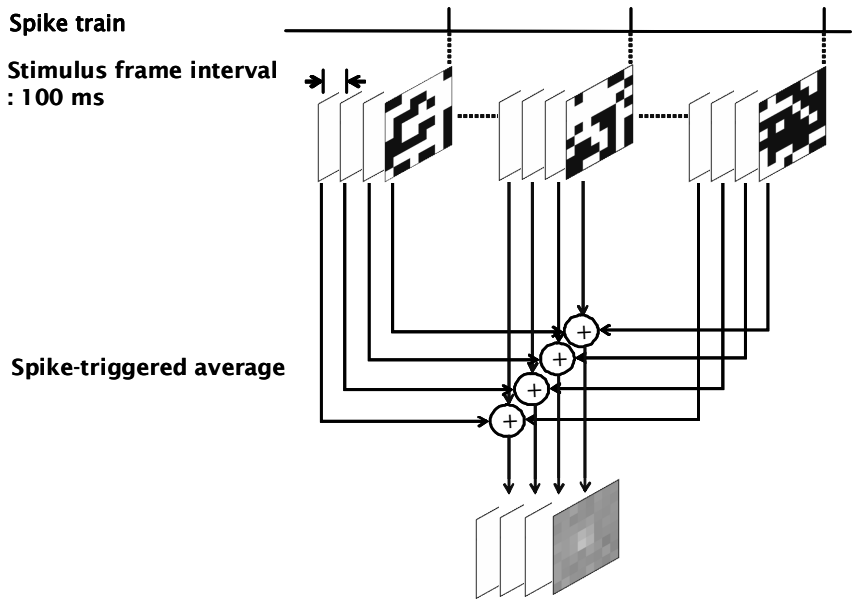

Fig. 2. Spike-triggered averaging of the random checkerboard stimulus. Each stack of stimulus frames represents 300 ms, 200 ms, 100 ms, and 0 ms preceding an action potential. These sequences were then aligned and ensemble averaged.

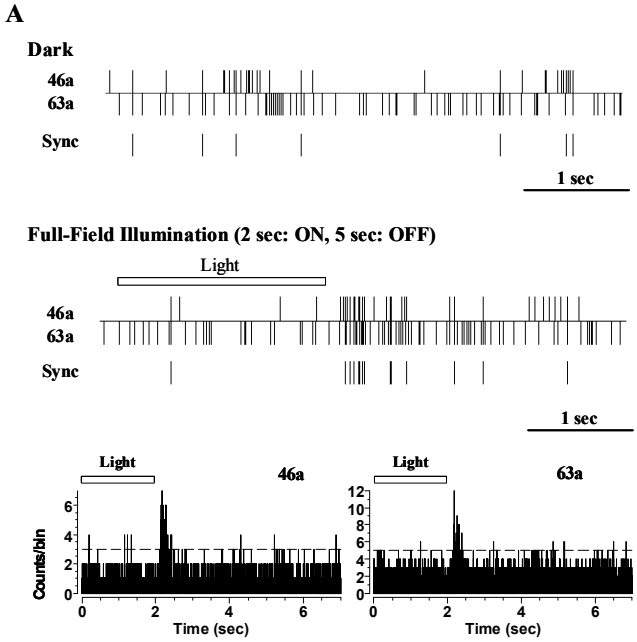

Fig. 3. Synchronous firing between nearby ganglion cells (46a, 63a). (A) Synchronized firing between two cells both in dark and full-field illumination are shown in raster plot. Sync raster was plotted when 63a cell fire spike within −5∼+5 ms from the 46a cell. With PSTH, 46a and 63a cells were identified as OFF cells. (B) Cross-correlation analysis between two RGC spike trains. Cross-correlogram of 46a and 63a showed narrow central peak both in dark and full-field illumination with white light (intensity 1.45 μW/cm^2), while the inset figure shows the cross-correlogram of the uncorrelated cells (46a and 62a). Dashed line indicates 99% confidence limits (bin: 1 msec).

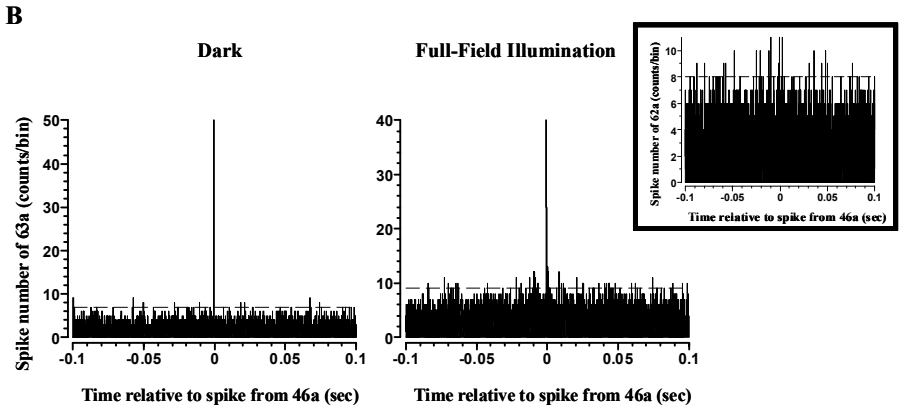

ing to pseudorandom sequence. The luminance of each pixel was independently updated every 100 ms for 9 minutes. After recording spike trains of RGC for 9 minutes with 5,400 frames of checkerboard, we calculated the spike-triggered average (STA) of the stimulus. It is pixelwise summation of light intensity (either 0 or 1) for each pixel of checkerboard stimuli, correlating with every spike divided by number of spikes recorded during 9 minutes. The basic technique used to map the receptive fields of retinal ganglion cells is illustrated in Fig. 2.

Data analysis

1. Analysis of spike activity

Each spike originated from single unit was sorted, and the spike train was time-stamped off-line by a spike extraction program (Off-line spike sorter; Plexon, Dallas, TX). From these data, raster plots and post-stimulus time histograms (PSTH) with light stimulus of 86 trials (recording time: 600 sec, ON: 2 sec, OFF: 5 sec, 600 sec/7 sec=86 trials) were obtained using Neuroexplorer (Plexon, Dallas, TX).

2. Cross-correlation analysis

From the spike trains, the patterns of interaction between two spike trains were studied by examining the cross-correlation function, which represents the firing rate of one neuron as a function of time before or after a spike from the other neuron. Flat cross-correlation function with time appears when two neurons fire independently, whereas a peak near zero time represents synchronous firing of

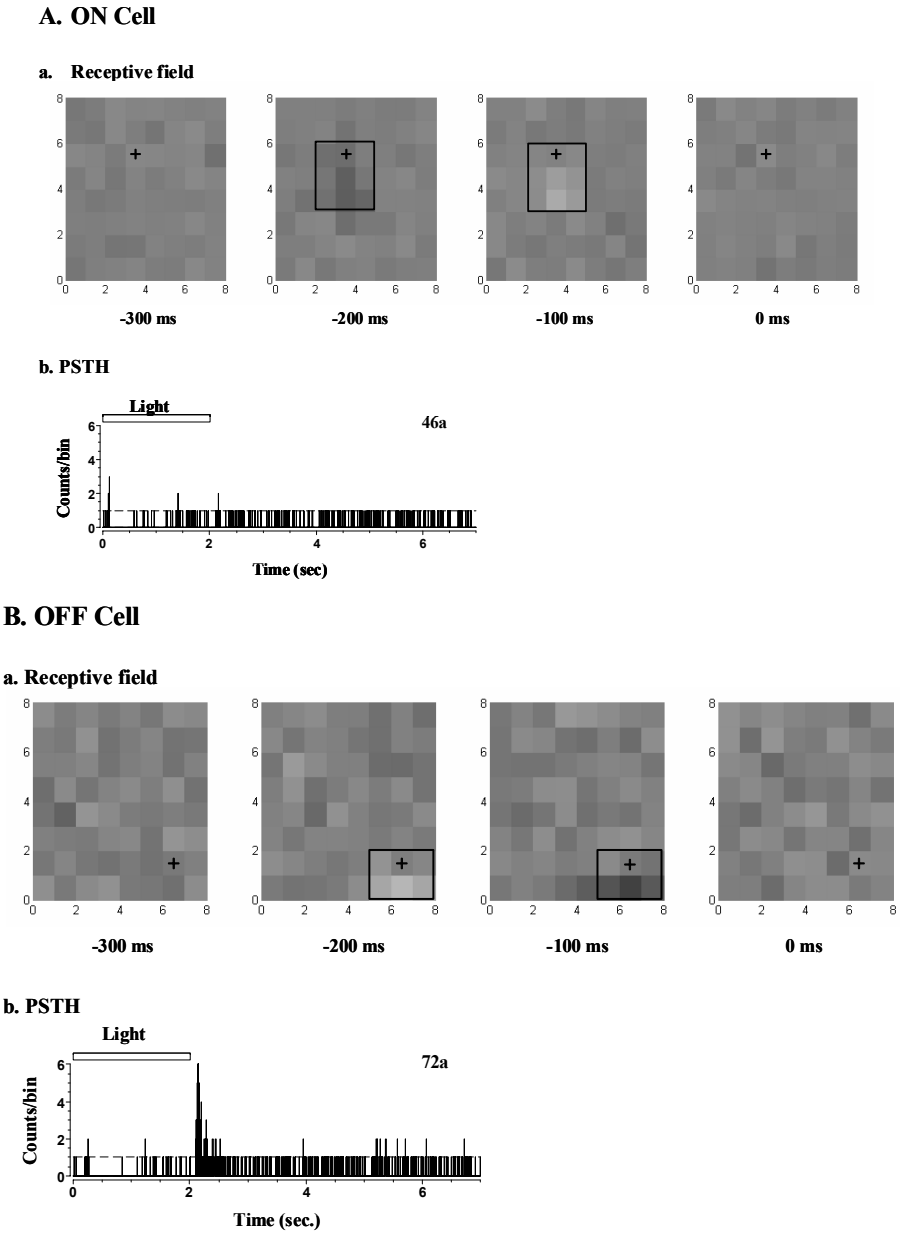

Fig. 4. Spatio-temporal receptive field of ON cell (A) and OFF cell (B). (A) a. Four frames of the spatio-temporal receptive field of ON cell are shown in succession to illustrate how the receptive field was evolved over time. Each frame shows spike-triggered average (STA) of stimulus, which preceded the action potential by the delay in milliseconds noted below each frame. The recording channel for RGC spike (channel 46) is marked by black cross. The boundary of STA of stimulus for this cell is marked by black line. Receptive field was determined by reverse correlation to flickering random checkerboard stimulation (pixel size: 200 μm, flicker interval: 100 ms, and mean intensity: 0.77 μW/cm^2). X and Y axis represent column and row of 8×8 MEA (0~8), respectively. b. This RGC was confirmed as ON cell by PSTH with light stimulus. (B) a. Four frames of the spatio- temporal receptive field of OFF cell are shown. The recording channel for RGC spike (channel 72) is marked by black cross. The boundary of STA of stimulus for this cell is marked by black line. b. This RGC was confirmed as OFF cell by PSTH with light stimulus.

these two neurons. The cross-correlation function between two spike trains was computed by histogramming all of the time differences between a spike from one cell and a spike from the other cell (NeuroExplorer; Plexon, Dallas, TX). Statistical significances were determined by the 99% confidence limits.

RESULTS

Synchronized firing

Fig. 3A illustrates firing of two RGCs in darkness and full-field illumination. By using the 46a cell (RGC activity detected by the electrode at the 4th column and the 6th row) as reference, we compared the firing of 63a cell. When the firing of 63a cell was within −5∼+5 ms of that of 46a cell, one time stamp was added in sync raster plot (The plot in 3rd row of dark and full-field illumination in Fig. 3A). Both 46a and 63a cells were identified as OFF cells. For more detailed analysis of firing, cross-correlation analysis between two cells was performed. The sharp peak at 0 ms delay indicates that these two cells fired synchronously (Fig. 3B). The narrow central peak changed little in the dark and full-field illumination of light. Differing from previous reports on cat (Mastronarde 1983), salamander (Brivanlou et al. 1998), and rabbit (DeVries, 1999), the broad hump next to the narrow central peak with light stimulus in cross-correlation function was not clearly seen. This difference will be discussed in the Discussion section.

Characterization of RGC pairs showing synchronized firing

Of 70 RGC pairs showing synchronized firing (number of retinas=9), we were able to characterize 33 pairs of RGCs. OFF-OFF cell pair, ON-ON cell pair, and ON/OFF −ON/OFF cell pair was 45.5% (15/33 pairs), 42.4% (14/33 pairs), and 12.1% (4/33 pairs), respectively. The other 37 pairs of RGCs could not clearly be characterized.

A ganglion cell's receptive field is defined as that region on the retinal surface in which a light stimulus produces a response. An example of a spatiotemporal receptive field is shown in Fig. 4 for an ON (brisk transient) cell and OFF cell. For ON (brisk transient) cell, the spike-triggered average (STA) of stimulus showed the transition from OFF (black pixels in the frames at 200 ms prior to the action potential) to ON (white pixels 100 ms prior to the action

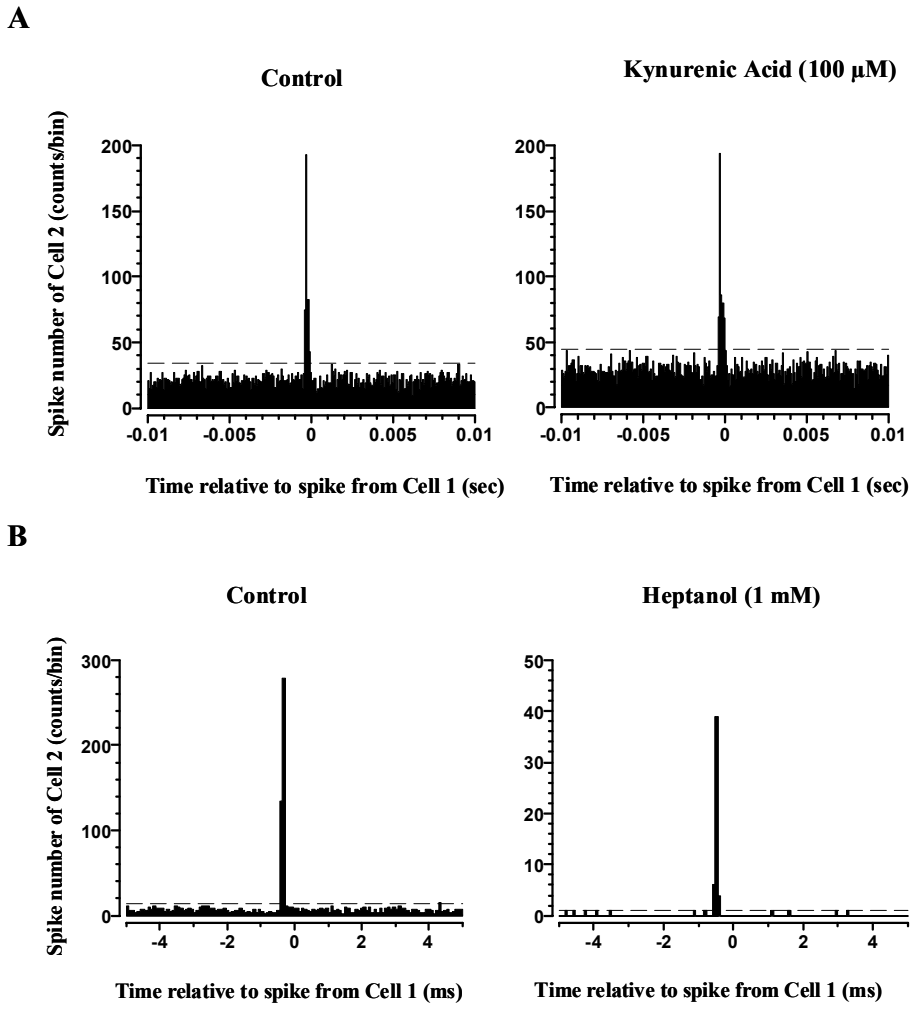

Fig. 5. Effects of kynurenic acid and heptanol on narrow correlation. (A) Narrow correlation persisted still when glutamate receptor was blocked with kynurenic acid (100 uM). Left: Control, Right: After treatment with kynurenic acid. (B) Narrow correlation was blocked with gap junction channel blocker, heptanol. The ordinate scale in left (Control) and right (Heptanol, 1 mM) is different. Dashed line indicates 99% confidence limits both in A and B (bin: 0.8 msec).

potential). For OFF cell, the STA of stimulus showed the transition from ON (white pixels in the frames at 200 ms prior to the action potential) to OFF (black pixels 100 ms prior to the action potential). In addition to temporal resolution, we could have spatial resolution for the STA of the stimulus.

Mechanism of synchronized firing

Since the synchronized firing between two cells (46a, 63a) occurred within −5∼+5 ms of time range (mostly −1∼+1 ms range), this could best be explained by the excitation of two RGCs through the gap junctions (Brivanlou et al, 1998), and our finding fits well the to classification of narrow correlation by Brivanlou et al. (1998). We tested the effect of gap junction blocker, heptanol, on the narrow correlation. Although milisecond range correlation seemed too short to be mediated chemically, we tested the effect of glutamate blocker, kynurenic acid, on the narrow correlation since the major input to RGC comes from bipolar cell through glutamatergic synapse. As expected, the narrow correlation was blocked with heptanol to 77±8.9% (n=10), while it persisted with kynurenic acid (n=7) (Fig. 5). The cell pairs showing narrow correlation in Fig. 5 were OFF -OFF cell pairs.

Table 1. Retinal ganglion cell pairs which show correlated firing whit different reference cell

Reference neuron	Target neuron	Reference neuron	Target neuron
45a	53a, 54b, 54c	63b	55b, 55a
45b	46b	64a	55a, 64c
46a	54b, 63a	64b	55a, 56a, 56b, 63a
46b	45b	64c	64a
52d	53a	65a	65b, 66a
53a	45a, 52d	65b	65a, 66a, 74a, 74b, 82a, 82b
54a	46b, 62a, 63a	66a	65a, 65b, 83a
54b	45a, 46a, 64a, 64b	74a	65b, 82a, 82b, 83a
54c	45a	74c	75a, 85b
55a	63a, 63b, 64a, 64b	75a	74a, 74c, 83a
56a	64b	82a	65b, 74a
56b	56c, 64b	82b	65b,74a,74b
56c	56b	83a	66a, 74a, 74b, 75a
62a	54a	84a	75a
63a	46a, 54a, 54b, 55a	85b	74c

Functional connectivity map of RGCs (Table 1. Fig. 6)

By changing the reference neuron, we could track down the target neurons which showed narrow correlation with the reference neuron (Table 1). Using this method, we could harvest 40 functional connectivity maps of RGCs (number of retinas=33) which showed the cluster of RGCs firing synchronously. Only the RGC which showed narrow correlation with at least 3 cells was included in the map. The maximum width and length of functional connectivity map never exceed 5 column widths and 5 row lengths; mostly 3 column widths and 5 row lengths (n=18). Two representative functional connectivity maps of RGCs are illustrated in Fig. 6. All the RGCs in Fig. 6 were OFF cells.

DISCUSSION

Narrow correlation

The results presented in detail here are based on a total of 1,155 RGCs and 160 cell pairs of correlated firing from 33 retinas. The results showed that there are correlated firing between RGCs occurring within −5∼+5 ms of time range (mostly ranging −1∼+1 ms), and that this narrow correlation was blocked by gap junction blocker, heptanol (n=10), but not by glutamatergic synapse blocker, kynurenic acid (n=9).

This narrow correlation corresponds well with results by others (Mastronarde, 1983; Brivanlou et al, 1998; DeVries,

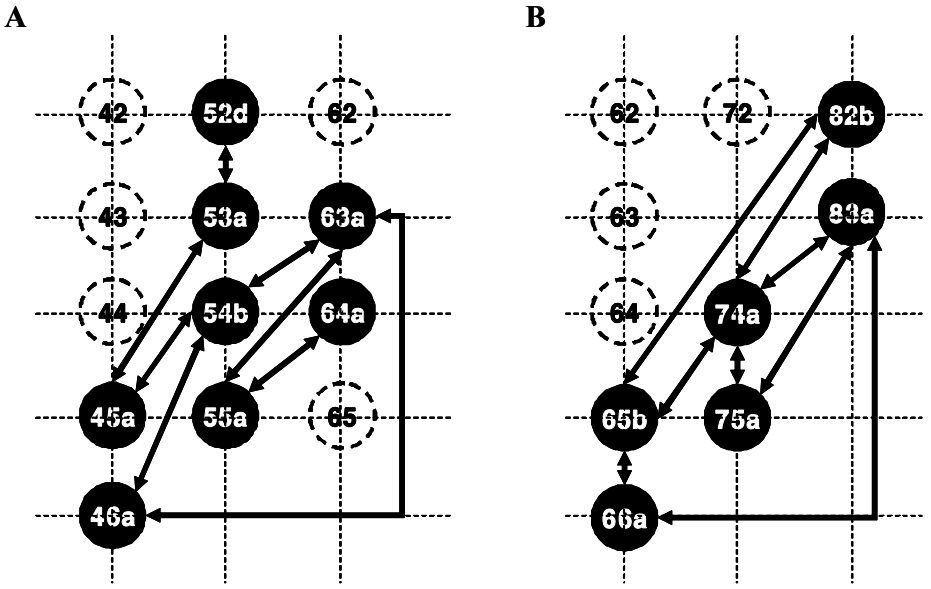

Fig. 6. Two representative functional connectivity maps of the cluster of RGCs firing together. (A) Functional connectivity map A. (B) Functional connectivity map B. The neuron 45a depicts the first cell recorded and sorted on the 4th column and the 5th row of 8×8 MEA. The correlated cells are drawn with closedcircles and connected with reciprocal arrows. These two functional connectivity maps were harvested from the same retinal preparation.

1999), however, a major difference was found in the fraction of narrow correlations. In the salamander retina, the spikes paired with millisecond synchrony constituted only a small fraction of each cell's spike train; on average, 8.1% of 61 cells (all types included) were involved in narrow correlations (Brivanlou et al, 1998). In the cat retina, Y cell action potential caused a spike in a coupled Y cell with a probability of only 1∼4% (Mastronarde, 1983). In our experiment with the rabbit retina, however, more than 14% of 160 cell pairs (all types included) were involved in narrow correlations. Possible explanation may reside in the gap junction channel density across species. Difference in the functional cell types might also be attributable. OFF cell pairs comprised 45.5% of all characterized pairs in our experiment, whereas 26% of cell pairs showed narrow correlation when OFF cells were restricted for correlated firing in the Brivanlou's study (1998). Therefore, more than 14% of narrow correlation is expected if we restrict cell pairs only to OFF-OFF pairs. The finding that only OFF cells, but not ON cells, exhibit rebound excitation (Margolis & Detwilder, 2007) is in good agreement with our results that the major cell types showing narrow correlation were OFF cell pairs.

In our experiment, the broad hump next to central peak was not observed with light stimulus, unlike other reports (Mastronarde 1983; Brivanlou et al, 1998; DeVries, 1999). This broad correlation is thought to be produced by light that activates photoreceptors the signals of which drive both recorded ganglion cells. Indeed, the temporal width of the broad correlation is similar to the duration of the dim flash response in dark-adapted rabbit rods (Nakatani et al, 1991). The possible explanation may be that our full-field illumination was not bright enough to activate photoreceptors. First, our full-field illumination was composed of 86 trials of ON (2 sec) and OFF (5 sec) protocol. Second, intensity of our ON stimulus (1.45 μW/cm^2) was in between medium (0.263 μW/cm^2 and bright (2.32 μW/cm^2) intensity of Meister et al's (1995). Even in their data, the broad hump next to central peak with medium light was not clear.

Characterization of RGC types: Receptive field map

Finding the STA of stimulus is based on the reverse correlation between RGC's response; e.g. action potential and the stimulus which drives the RGC to fire the action potential. Here, we provided the spatio-temporal receptive field maps of ON cell and OFF cell. The reason for measuring the receptive field was that the receptive field is basic component to understand the sensory neuron. Even if there was OFF to ON transition for ON cell (ON to OFF transition for OFF cell) in 200 ms and 100 ms before the action potential, respectively, the resolution power for transition was lower than those by others (Meister et al, 1995; Brown et al, 2000). For receptive field reconstruction, we used about 500 action potentials of each specific RGC recorded during 540 sec, while Meister et al. used 9,738 action potentials recorded for 4,300 sec. The use of too small number of action potentials in our experiment might have been a reason for low resolution power. The second possibility may reside in the low frequency of flicker stimulus (our 10 Hz vs Brown's 70 Hz). The third possibility is the chance that we might have missed the right frame, since we performed spike-triggered averaging only for 300 ms, 200 ms, 100 ms, and 0 ms before the action potential. We should have done spike triggered averaging over the stimulus segment of 1 second duration preceding each action potential, since the overall integration time of the retina is generally less than 1 second.

Implication of functional connectivity map of RGCs as a useful tool of stimulation encoding strategy for the retinal prosthesis

By cross-correlation analysis, we harvested 40 functional connectivity maps which showed the cluster of RGCs with narrow correlation. We suggest this map as a useful tool for stimulation encoding strategy for the retinal prosthesis, since stimulating each cluster would be more efficient than separately stimulating each individual RGC.

The maximum width and length of functional connectivity map never exceeded 5 column widths and 5 row lengths, mostly 3 column widths and 5 row lengths (n=18), which provides a good guideline for how to apply optimal electrical stimulation; e.g. electrical stimulation through every three columns and every five rows of MEA.

We are currently in the process to figure out in detail the properties of functional connectivity map of RGCs.

ACKNOWLEDGEMENT

This work was supported by grants of Ministry of Health & Welfare (A050251), ERC Program of MEST/ KOSEF (R11-2000-075-01002-0).

REFERENCES

Amthor FR, Takahashi ES, Oyster CW. Morphologies of rabbit retinal ganglion cells with concentric receptive fields. *J Comp Neurol* 280: 72−96, 1989a

Amthor FR, Takahashi ES, Oyster CW. Morphologies of rabbit retinal ganglion cells with complex receptive fields. *J Comp Neurol* 280: 97−121, 1989b

Arnett D, Spraker TE. Cross-correlation analysis of the maintained discharge of rabbit retinal ganglion cells. *J Physiol (London)* 317: 29−47, 1981

Brivanlou IH, Warland DK, Meister M. Mechanisms of concerted firing among retinal ganglion cells. *Neuron* 20: 527−539, 1998

Brown SP, He S, Masland RH. Receptive field microstructure and dendritic geometry of retinal ganglion cells. *Neuron* 27: 371−383, 2000

Caldwell JH, Daw NW. New properties of rabbit retinal ganglion cells. *J Physiol (Lond.)* 276: 257−276, 1978

DeVries SH, Baylor DA. Mosaic arrangement of ganglion cell receptive fields in rabbit retina. *J Neurophysiol* 78: 2048−2060, 1997

DeVries SH. Correlated firing in rabbit retinal ganglion cells. *J Neurophysiol* 81: 908−920, 1999

Egert U, Schlosshauer B, Fennrich S, Nisch W, Fejtl M, Knott T, Muller T, Hammerle H. A novel organotypic long-term culture of the rat hippocampus on substrate-integrated multielectrode arrays. *Brain Res Protoc* 2: 229−242, 1998

Guenther E, Herrmann T, Stett A. The retina sensor: An in vitro tool to study drug effects on retinal signaling. In: Taketani M, Baudry M, ed, *Advances in Network Electrophysiology Using Multi-electrode Arrays*. 1st ed. Springer, New York, p 321−331, 2006

Humayun MS, Weiland JD, Fujii GY, Greenberg R, Williamson R, Little J, Mech G, Cimmarusti V, Boemel GV, Dagnelie G, de Juan Jr E. Visual perception in a blind subject with a chronic microelectronic retinal prosthesis. *Vis Res* 43: 2573−2581, 2003

Lowenstein JI, Montezuma SR, Rizzo III JF. Outer retinal degeneration: an electronic retinal prosthesis as a treatment strategy. *Archives of Ophthalmology* 122: 588−596, 2004

Margolis DJ, Detwilder PB. Different mechanisms generate maintained activity in ON and OFF retinal ganglion cells. *J Neurosci* 27: 5994−6005, 2007

Mastronarde DN. Interactions between ganglion cells in cat retina. *J Neurophysiol* 49:350−365, 1983.

Meister M, Pine J, Baylor DA. Multi-neuronal signals from the retina: acquisition and analysis. *J Neurosci Methods* 51: 95−106, 1994

Meister M, Lagnado L, Baylor DA. Concerted signaling by retinal ganglion cells. *Science* 270: 1207−1210, 1995

Meister M. Multineuronal codes in retinal signaling. *Proc Natl Acad Sci USA* 93: 609−614, 1996

Meister M, Berry MJ 2nd. The neural code of the retina. *Neuron* 22: 435−450, 1999

Nakatani K, Tamura T, Yau KW. Light adaptation in retinal rods of the rabbit and two other nonprimate mammals. *J Gen Physiol* 97: 413−435, 1991

Rizzo JF III, Wyatt J, Lowenstein J, Kelly S, Shire D. Perceptual efficacy of electrical stimulation of human retina with a microelectrode array during short-term surgical trials. *Invest Ophthalmol Vis Sci* 44: 5362−5369, 2003

Seo J, Zhou J, Kim E, Koo K, Ye JH, Kim SJ, Chung H, Cho DD, Goo YS, Yu YS. A retinal implant system based on flexible polymer microelectrode array for electrical stimulation. In: Tombran-Tink J, Barnstable C, Rizzo JF ed, *Visual Prosthesis and Ophthalmic Devices: New Hope in Sight*. 1st ed. Humana Press Inc, New Jersey, p 107−119, 2007

Stett A, Barth W, Weiss S, Haemmerle H, Zrenner E. Electrical multisite stimulation of isolated chicken retina. *Vis Res* 40: 1785−1795, 2000

Zrenner E, Besch D, Bartz-Schmidt KU, Gekeler F, Gabriel VP, Kuttenkeuler C, Sachs H, Saier H, Wilhelm B, Wilke R. Subretinal chronic multi-electrode arrays implanted in blind patients. *Invest Ophthalmol Vis Sci* 47: E-Abstract 1538, 2006